Influence of a bulk superconducting environment on the superconductivity of one-dimensional zinc nanowires

Mingliang Tian, Nitesh Kumar, Jinguo Wang, Shengyong Xu, and Moses H. W. Chan
The Center for Nanoscale Science and Department of Physics, The Pennsylvania State University, University Park, Pennsylvania 16802-6300, USA

(Received 8 March 2006; revised manuscript received 8 June 2006; published 26 July 2006)

In an earlier paper [Tian *et al.*, Phys. Rev. Lett. **95**, 076802 (2005)], we reported an antiproximity effect (APE) in a system consisting of 40 nm diameter Zn nanowires (ZNWs) sandwiched between bulk Sn and In electrodes. When the electrodes are in the superconducting state, the superconductivity of the ZNWs is suppressed. When the electrodes are driven normal by a magnetic field, the superconductivity of the ZNWs recovers. In this paper we report systematic transport studies of this phenomenon with ZNWs sandwiched between Pb electrodes. The APE found in this system is subtle, showing up primarily in significantly reducing the critical current of the ZNWs when the Pb electrodes are in a superconducting state. The critical current is independent of the magnetic field until it is increased to a characteristic value H^d near 0.6 kOe when the critical current shows a rapid enhancement and reaches a maximum value at the critical field of Pb electrodes at 0.94 kOe.

DOI: 10.1103/PhysRevB.74.014515 PACS number(s): 73.63.Nm, 74.45.+c, 74.78.Db

I. INTRODUCTION

A normal metal (N) acquires superconducting properties in the presence of a nearby superconductor (S), a phenomenon known as the superconducting proximity effect.[1–3] This phenomenon is thought to be related to Andreev reflection[1,4] that converts a normal current to a supercurrent at the SN interface. When a superconductor (S) is connected to another superconductor (S') forming a SS' structure, such a combined SS' system at temperatures below the critical temperatures (T_c) of both S and S' can be considered as a composite superconductor with a continuous superconducting order parameter through the interface. However, if a barrier layer (such as a metal, semiconductor, or insulator) is introduced at the interface between S and S', the combined structure can be either a superconducting weak link or a Josephson tunneling junction depending on the height of the barrier potential.[5–7] The constriction system that comprises of a superconducting stripe of micrometer-size in diameter between two macroscopic superconductors of the same material (without a barrier layer between the stripe and the macroscopic superconductor) is another weak-link superconductor system. The properties of such a constriction system are related to the length (L) of the stripe. If the length of the stripe is smaller than $\xi(0)$, the superconducting coherence length, its superconductivity, compared with an individual longer wire [$L \gg \xi(0)$], was found to be enhanced through the coupling to the two strong superconducting reservoirs.[8]

There are a number of recent experiments studying the transport properties of superconducting nanowires (SNWs).[9–23] The diameters of these SNWs range from a few to tens of nanometers, on the order or smaller than the superconducting coherence length $\xi(0)$ and penetration depth $\lambda(0)$. Not surprisingly the transport properties of these SNWs exhibit one-dimensional (1D)-like behavior. Nonzero finite resistance found below the superconducting transition temperature in these nanowires has been attributed to thermally activated phase slips[16,17,24] and quantum phase slip processes.[18–23,25,26] A number of recent theoretical papers[27–29] proposed that the superconductivity in these 1D quantum nanowires depends strongly on how the nanowires are coupled to the external environment. There have not been extensive systematic experimental investigations to test these proposals. Recently, we reported measurements on a system consisting of Zn nanowires (ZNWs) of 40 nm in diameter sandwiched between two bulk superconductors (Sn or In).[9] In such systems, namely, Sn/ZNWs/Sn and In/ZNWs/In, we found a behavior that is completely unexpected. The superconductivity of ZNWs is found to be suppressed either completely or partially by the superconducting electrodes. When the bulk electrodes are driven into their normal state by an external magnetic field (H), the superconductivity of the ZNWs is recovered. This unusual phenomenon is named the "antiproximity" effect (APE). The APE observed in wires of 40 nm in diameters is not found in ZNWs with diameters equal to or larger than 70 nm. The strength of the APE depends on the length of the ZNWs, the resistance of the interface between the nanowires, and the bulk electrodes, but does not appear to depend on the number of ZNWs sandwiched between the electrodes. The strength also depends on the materials of the electrode, i.e., with Sn as bulk electrodes, the superconductivity in 40 nm ZNWs of 6 μm in length is found to be completely suppressed, while the suppression is partial for wires of the same length with In electrodes.[9]

In this paper, we report a systematic study of the APE with bulk Pb as electrodes. The Pb-induced APE is found to be even weaker than that using In as electrodes. There is no sign of APE in the resistance (R) versus temperature (T) scan at low excitation current through the transition temperature of Zn. However, measurements of the voltage-current (V-I) characteristics of the Pb/ZNWs/Pb system at different magnetic fields show evidence of APE. Specifically, the critical current (I_c) of ZNWs with Pb in the superconducting state is significantly reduced as compared with Pb in the normal state. The critical current is essentially independent of magnetic field H until H is increased to an "onset" field H^d at

which the I_c increases steeply with H. This "onset" magnetic field H^d ($H^d < H_c^{Pb}$) appears to play a role in decoupling the ZNWs from the superconducting electrodes. The findings reported in this paper corroborate and complement our earlier report[9] and provide a consistent experimental picture of this fascinating phenomenon.

This paper is organized as follows: synthesis and structural characterization of Zn nanowires used in this work are described in Sec. II. Transport measurements (*R-T*, *R-H*, and *V-I* curves) of Pb/ZNWs/Pb systems are presented in Sec. III. Several possible models that might be relevant to our data are discussed in Sec. IV. A brief conclusion is shown in Sec. V.

II. SYNTHESIS AND CHARACTERIZATION OF Zn NANOWIRES

ZNWs used in Ref. 9 and in this study were fabricated by electrochemically depositing Zn into the open channels of commercially available "track-etched" porous polycarbonate (PC) membrane (Structure Probe, Inc., USA).[30–32] The open channels in these membranes are aligned parallel to each other and perpendicular to the surface of the membrane within a dispersion of 17°. The pore density of a PC membrane is about 6×10^8 pores/cm^2, but pores are distributed randomly. The electrolyte was prepared by dissolving 4.7 g $ZnCl_2$ into 200 ml distilled water, and then mixed with 40 ml saturated KCl and 0.5 g gelatin. Deposition was made at room temperature under a constant voltage between −0.1 and −0.4 V with a pure bulk Zn wire as the anode. A Au film evaporated on one side of the membranes serves as the conducting cathode. The actual diameter of the resultant nanowires by using PC membranes is usually several times larger than the pore size quoted by the manufacturer.[31] We obtained 40 and 70 nm diameter nanowires using PC membranes with quoted pore sizes of 10 and 30 nm. This is because the pore diameter on one end of the channels of the PC membrane is smaller than the inner pore diameter (the quoted pore size may be reasonable for the purpose of filtration). The morphology and microstructures of the resulting nanowires were characterized by a JEOL 2010F field-emission transmission electron microscopy. The ZNW specimen was prepared by dissolving the PC membrane in dichloromethane, and then a drop of the solvent with freestanding nanowires in suspension was placed on a Lacey carbon grid.

Figures 1(a) and 1(b) show transmission electron microscopy (TEM) images of ZNWs at two different magnifications. The majority of ZNWs has a bamboolike morphology with an elongated crystalline segments ranging in length from the wire diameter (40 nm) to micrometers. Three main growth orientations, [0001], [01$\underline{1}$0], and [1$\underline{2}$10], are observed from randomly selected ZNWs.[32] Figure 1(c) shows a ZNW with a growth direction of [0001]. The selected area electron diffraction pattern is shown in the inset of Fig. 1(c). A ZnO layer of 2–3 nm in thickness is always found on the surface of a ZNW. This oxide layer may have formed after the nanowires were released from the membrane. Locally enlarged high resolution TEM image of the interface between the Zn nanowire and the ZnO layer is shown in Fig. 1(d). The growth of Zn and ZnO show an epitaxial relationship but dislocations at the Zn/ZnO interface and the defects in the Zn wires are expected because of the lattice mismatch between Zn and ZnO. The misfits between Zn and ZnO along [0001], [01$\underline{1}$0], and [1$\underline{2}$10] orientations are 5.2%, 21.6%, and 21.6%, respectively.[32]

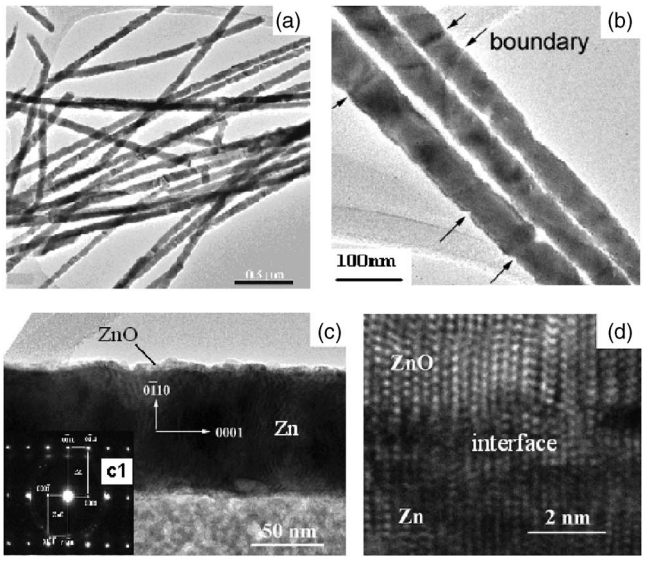

FIG. 1. (a) and (b) show the TEM images of the ZNWs. (c) shows growth direction [0001], observed in a randomly selected ZNW. The selected area electron diffraction pattern is shown in the inset. (d) shows locally enlarged high resolution TEM image of the interface between Zn and the ZnO.

III. MEASUREMENTS OF SUPERCONDUCTIVITY ON Pb/ZNWs/Pb COMBINATIONS

Transport measurements were carried out with a physical properties measurement system, equipped with a ^{3}He insert and a superconducting magnet. Because the ZNWs oxidize easily when they are released from the membrane, electrical transport measurements were made on the ZNW array still embedded inside the membrane. Current and voltage electrodes for the measurements were made by mechanically squeezing high-purity superconducting Pb wires of 0.5 mm diameter onto the two sides of the PC membrane forming a Pb/ZNWs/Pb structure [a schematic of the configuration is shown in the inset of Fig. 2(a)]. The pre-evaporated Au layer on the membrane was wiped away while the membrane is submerged in pure ethanol before the 0.5 mm diameter superconducting wires (or electrodes) were squeezed onto the membrane. The PPMS ^{3}He refrigerator is particularly suitable for carrying out transport measurements on these structures because the entire procedure in making electrical contacts onto a freshly fabricated sample and securing the sample to the cooling stage in vacuum can be accomplished within 1–3 min. The sample can be cooled down to a helium temperature in a matter of a few hours. Details of our technique for transport measurements can be found in Refs. 9 and 19. The total R measured with this configuration consists of the contributions of Pb electrodes, ZNWs, and ZNWs/Pb

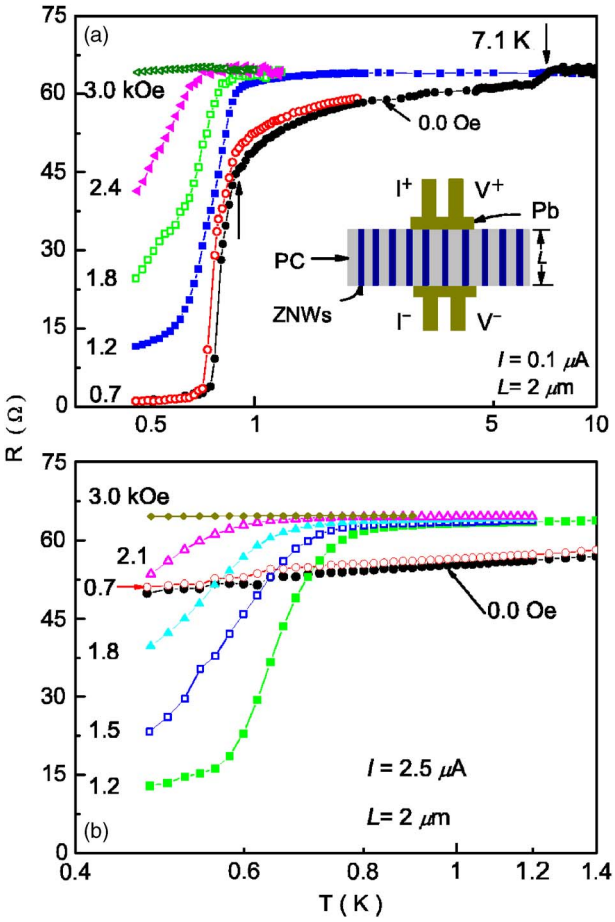

FIG. 2. (Color online) R-T curves of ZNWs (d=40 nm, L =2 μm) with Pb electrodes, measured at different magnetic fields aligned perpendicular to the wire axis. (a) Excitation current, I =0.1 μA; (b) I=2.5 μA.

interface. The number of ZNWs contacting the Pb electrodes depends on the squeezing pressure and the filling factor of the membrane. It ranges from as few as a single wire to as many as several tens of wires.

The residual resistance ratios (RRR), R(300 K)/R(8 K), of all our ZNW samples falls between 1.5 and 1.9. The value of the RRR is 5–6 times smaller than that of single-crystal Sn nanowires of the same diameter.[19] The superconducting coherence length $\xi(0)$ and electron mean free path ℓ_e of ZNWs are estimated, respectively, to be about 155 and 12 nm.[9] Dislocations and other defects in the nanowires formed either during electrochemical deposition and/or while the electrodes were mechanically squeezed onto the membrane are the likely origins for the reduced RRR and a ℓ_e smaller than the wire diameter.

Compared with bulk Sn and In, bulk Pb has a higher T_c (7.2 K) and critical field H_c (~803 Oe) (Ref. 33) but a shorter coherence length $\xi(0) \sim 83$ nm. The Pb/ZNWs/Pb system used in this paper is prepared by placing 40 nm diameter ZNWs of 2 μm in length between two bulk Pb superconductors. Figure 2(a) shows R-T curves measured at a dc excitation current of 0.1 μA under different H, aligned perpendicular to the wire axis. The RRR=R(300 K)/R(8 K), of this nanowire array is about 1.7, almost the same as that of ZNWs with bulk Sn and In electrodes reported previously.[9] The number of ZNWs making contact to the Pb electrodes is estimated to be ~5, following the reasoning of Ref. 9. The critical field H_c^{Pb} of Pb electrodes in this sample, determined from the R-H measurement (see Fig. 5), is around 0.94 kOe at 0.47 K, higher than the bulk value reported previously. This enhancement is probably related to strains in the Pb electrodes induced by squeezing. At H =0 kOe, the R-T curve shows a small resistance drop at 7.1 K and then a larger drop near 0.9 K. These resistance drops have their origins in the superconducting transitions of Pb electrodes and ZNWs, respectively. A finite resistance of the order of 1.0 Ω is also found down to 0.47 K at H =0 Oe. When the bulk Pb electrodes are completely driven to the normal state by a magnetic field H=1.2 kOe, the R-T curve shows only one drop near 0.85 K due to the superconducting transition of the ZNWs. The slight reduction of T_c from 0.9 to 0.85 K at 1.2 kOe is due to the presence of the magnetic field. The onset temperature thereafter decreases with increasing H and becomes lower than 0.47 K at a field of 3.0 kOe. The overall features of the R-T curves resemble those found in the 70 nm diameter ZNWs with bulk Sn or In electrodes where the ZNWs and electrodes both show superconductivity at their respective T_c.[9] There is no indication of the APE in these R-T curves measured at 0.1 μA. However, if the excitation current is increased from 0.1 to 2.5 μA, the R-T curves at H=0 kOe and at 0.7 kOe do not show any sign of superconductivity of the ZNWs [Fig. 2(b)]. Upon the application of a magnetic field of 1.2 kOe that drives the Pb electrodes normal, a sharp resistance drop appears near 0.85 K. These features show APE and resemble the R-T curves obtained in our previous 40 nm diameter ZNW samples with Sn or In electrodes.[9]

The puzzling results of Figs. 2(a) and 2(b) become sensible when we examine the V-I curves at low temperatures as a function of the magnetic field. Figures 3(a) and 3(b) show the V-I characteristics at 0.47 K at different magnetic fields below 0.97 kOe, the critical field of Pb electrodes. Figures 3(c) and 3(d) show curves for fields above the critical field of Pb up to 3.5 kOe. Two characteristic values I_{c1} and I_{c2}, namely the lower and upper critical current, can be defined from these V-I curves. Above I_{c2} the nanowires are fully in the normal state. Below I_{c1}, the nanowires are "nominally" in superconducting states with a small finite resistance. The V-I curve below I_{c1} is linear in the log-log plot of Fig. 3(b) and parallel to the curve of nanowires in a normal state. This indicates that the small finite resistance below I_{c1} is Ohmic over the excitation current range from I_{c1} down to 10 nA, the limit of our measurement system. The origin of this small nonzero finite resistance below I_{c1} will be discussed later. Between I_{c1} and I_{c2}, the ZNWs are in the transition region between the superconducting and normal state where the resistance is strongly excitation current dependent. The critical currents I_{c1} and I_{c2} are essentially independent of the magnetic field up to H=0.6 kOe (they are, respectively, 1.6 and 2.2 μA). Under a magnetic field between 0.6 and 0.9 kOe when the Pb electrodes are still superconducting, both I_{c1} and I_{c2}, contrary to the behavior of "standard" superconducting system, actually increase with increasing applied magnetic fields until 0.9 kOe. With a further increase in magnetic

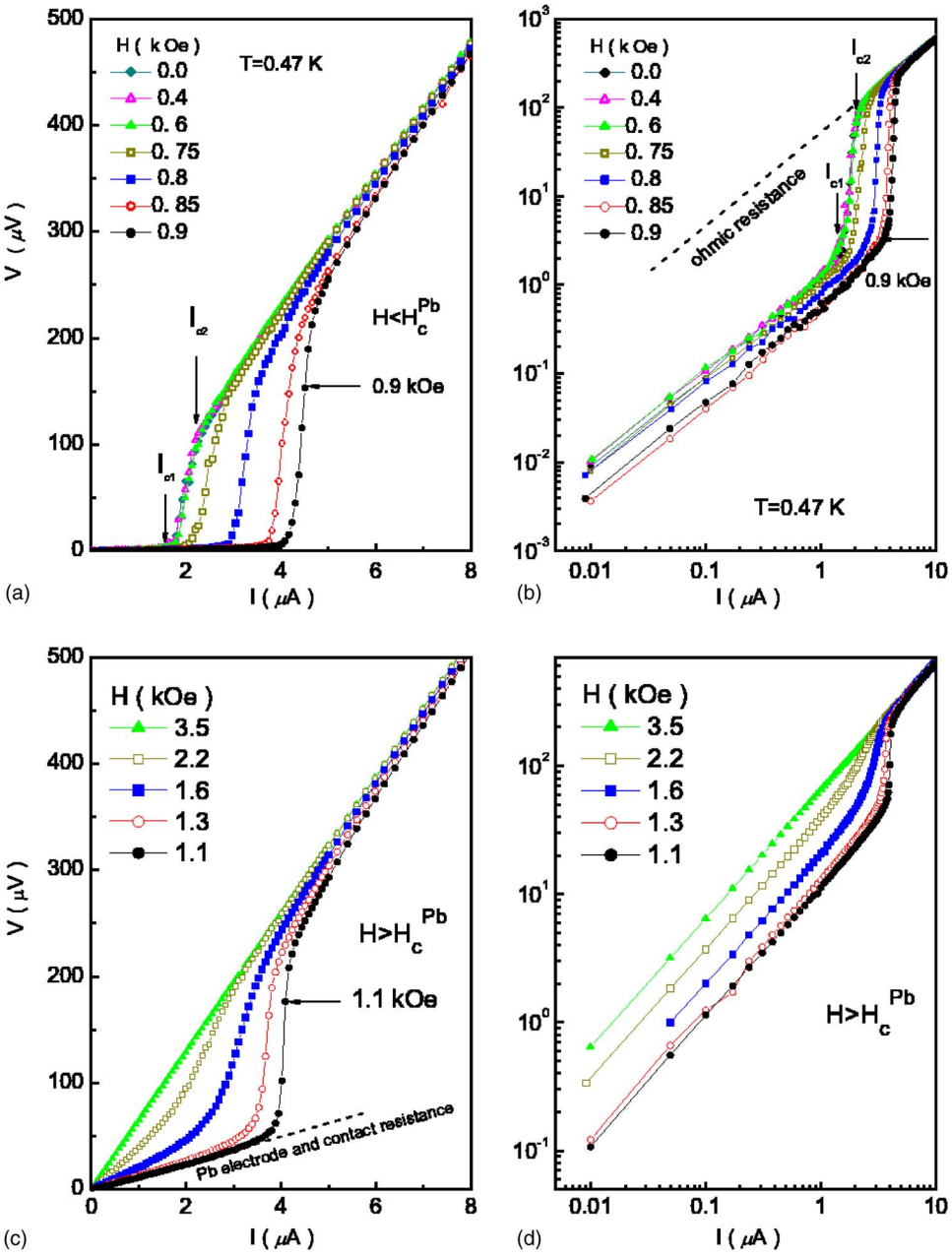

FIG. 3. (Color online) *V-I* characteristics of ZNWs with Pb electrodes, measured at 0.47 K at different magnetic fields, (a) *V-I* curves in linear scale at $H < H_c^{\mathrm{Pb}}$ and the same data in the log-log scale are shown in (b) (the dashed line indicates the normal state Ohmic *V-I* curve); (c) *V-I* curves in a linear scale at $H > H_c^{\mathrm{Pb}}$ (the dashed line indicates the Ohmic finite resistance due to the Pb electrodes and interfaces), and the same data in the log-log scale are shown in (d).

fields beyond the H_c^{Pb} of Pb, both I_{c1} and I_{c2} start to decrease with increasing magnetic fields, assuming the standard behavior. Because of the small diameter of ZNWs, their critical magnetic field far exceeds the bulk value (~50 Oe) and reaches about 3.0 kOe at $T=0.47$ K. The higher finite resistance (~10 Ω), indicated by the dashed line in Figs. 3(c) and 3(d) below I_{c1} under a field of 1.1 kOe is primarily due to the normal Pb electrodes and Pb/ZNWs interfaces. These data implied that the superconductivity of ZNWs is weakened by the existence of superconducting Pb reservoirs.

The critical currents I_{c1} and I_{c2} deduced from Fig. 3 are plotted versus H at 0.47 K in Fig. 4. A sharp enhancement of I_{c1} (I_{c2}) from 1.6 μA (2.2 μA) to 3.8 μA (4.8 μA) is found in a magnetic field range between 0.6 and ~0.9 kOe. This unusual dependence of the critical current on the magnetic field makes it easy to understand the *R-T* curves shown in Fig. 2. In Fig. 2(b), the ZNWs do not show superconducting transition below 0.7 kOe because the excitation current (2.5 μA) exceeds the upper critical current I_{c2} in this magnetic field region. Similarly, the recovery of superconductivity at a higher magnetic field of $H \geqslant 1.2$ kOe is because the excitation current (2.5 μA) falls below the upper critical current (I_{c2}) in that magnetic field region. If an excitation current less than the lower critical current I_{c1} at 0.47 K (~1.6 μA) is used, as it is the case for the scans shown in Fig. 2(a), then the sample shows superconducting behavior irrespective of whether the Pb electrodes are superconducting or normal. We shall show below that the reduction of the critical current by the superconducting Pb electrodes on the ZNWs is another manifestation of the APE found with Sn and In electrodes.

Figure 5(a) shows *R-H* scans at 0.47 K, measured at four different excitation current, 0.1, 3, 4.0, and 11 μA. At an excitation current of 11 μA, higher than the maximum criti-

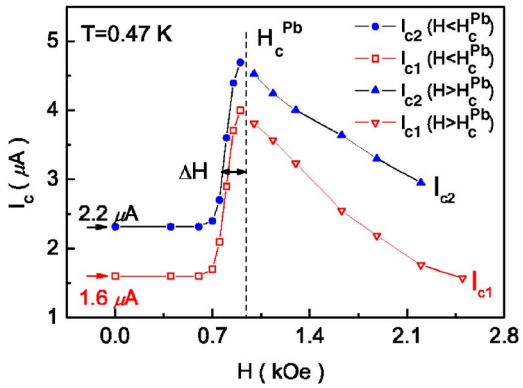

FIG. 4. (Color online) The low and upper critical current (I_{c1} and I_{c2}) versus magnetic field H at 0.47 K.

cal current of 4.8 μA (see Fig. 4), the ZNWs are in the normal state at all magnetic fields. A resistance jump is found between 0.94 and 1.0 kOe, indicating the superconducting to normal transition of Pb electrodes. The onset field of 0.94 kOe is defined as the critical field H_c^{Pb} of Pb electrodes in this paper. The R-H curves measured at 3.0 and 4.0 μA are more interesting as these values fall below the upper critical current over a range of magnetic fields (Fig. 4), in which the system will show low resistance. Indeed these curves show a sharp resistance drop from about 55 Ω down to about 1.0 Ω that commence at H^d=0.65 kOe for the 3.0 μA curve and 0.75 kOe for the 4.0 μA curve. The resistance remains at these low values until the field is raised to 0.94 kOe, the H_c^{Pb} of Pb electrodes. Figure 5(b) with R plotted in the log scale over a narrower range in H highlights the

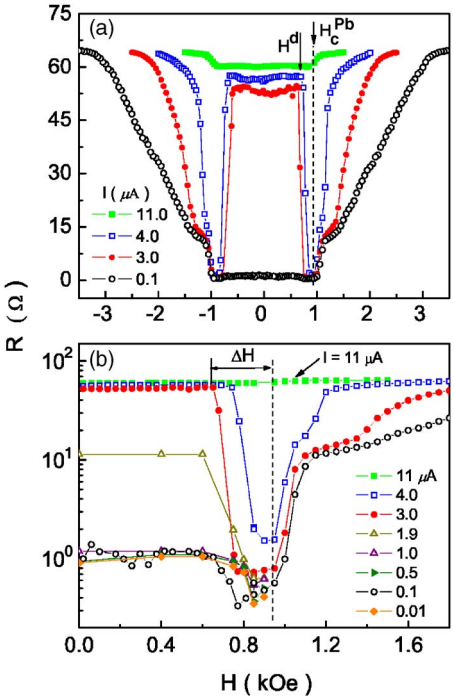

FIG. 5. (Color online) R-H curves at 0.47 K, measured at a different excitation current (I). (a) Both axes in the linear scale and (b) R axis in the log scale in highlighting the results in a low resistance region. The H_c^{Pb} of Pb electrodes is indicated by the dashed line.

results in low resistance region. Four additional curves at I =10 nA, 0.5, 1.0, and 1.9 μA are added to this plot, where the resistance at specific magnetic field values were deduced from the V-I curves shown in Fig. 3(b). The R-H curve at 1.9 μA resembles that at 3.0 and 4.0 μA, except that the resistance at the low magnetic field region of $H<H^d$ (~0.6 kOe) is lower. The reason for the lower resistance at low fields is because 1.9 μA lies between I_{c1} (~1.6 μA) and I_{c2} (2.2 μA) below 0.6 kOe. R-H curves measured at different temperatures at a fixed excitation current of 2.1 μA are shown in Fig. 6. This figure complements Fig. 5. A switching of the ZNWs from the normal (or high resistance) to the superconducting state at H^d and minimum in R between H^d and H_c^{Pb} are again clearly displayed.

The R-H curves measured at an excitation current well below the critical current I_{c1} (~1.6 μA) at H=0 Oe display perhaps the most interesting behavior. Figure 5(b) showed that between 0 and 0.6 kOe the resistance measured in the low current limit (at 10 nA, 0.1, 0.5, and 1.0 μA) is independent of the current (Ohmic) with a value of 1.0 Ω. Interestingly, when the field is increased beyond 0.6 kOe, the resistance begins to drop with the magnetic field reaching a minimum of 0.35 Ω before showing a steep increase at the H_c^{Pb}, similar to the behavior of the R-H scans measured at 1.9, 3.0, and 4.0 μA. The fact that a minimum in R is found over the same magnetic field range at such a low excitation current means that the H^d, the field value at which R begins to drop, is an important characteristic magnetic field in controlling the properties of the Pb/ZNWs/Pb system. While the exact mechanism is still not yet known, it seems clear that the various manifestations of the APE we have observed in Sn/ZNWs/Sn, In/ZNWs/In, and Pb/ZNWs/Pb systems have their origin in the coupling of the superconducting order pa-

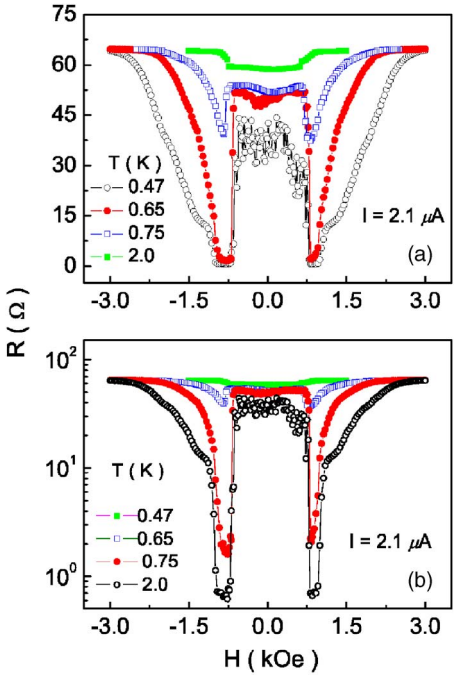

FIG. 6. (Color online) R-H curves measured at different temperatures with an excitation current 2.1 μA. (a) Both axes in a linear scale and (b) R axis in a log scale.

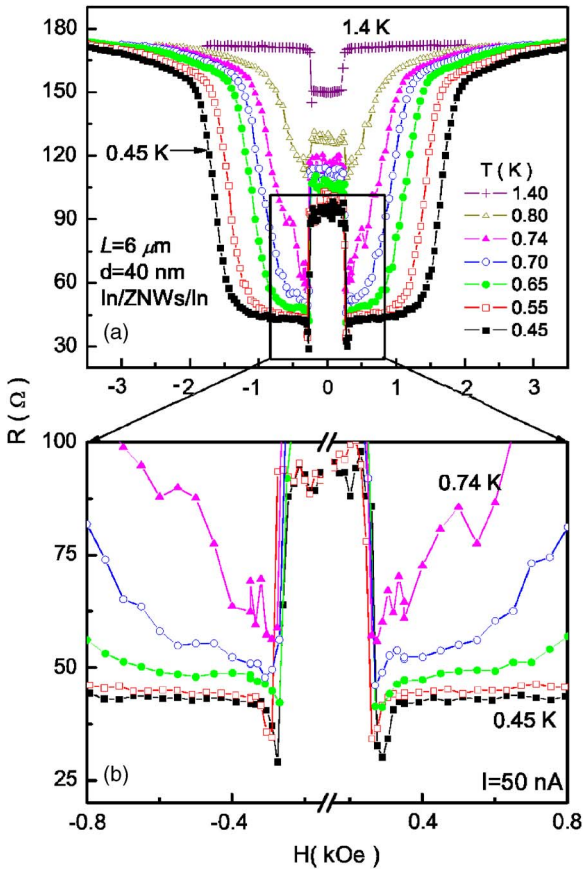

FIG. 7. (Color online) (a) shows *R*-*H* scans of ZNWs with In electrodes ($L=6$ μm, $d=40$ nm) at different temperatures. In this sample, the bulk In electrodes show an incomplete suppression effect on the superconductivity. In this case, a minimum in R was observed near a magnetic field 0.25 ± 0.01 kOe, just below the H_c of In electrodes when $T<0.7$ K. A locally enlarged part of this plot is shown in (b).

rameters of the bulk electrodes and the ZNWs. The H^d observed in the Pb/ZNWs/Pb system can be considered as a critical decoupling field. Above H^d, the coupling between Pb electrodes and the ZNWs becomes significantly weakened and the ZNWs become a more robust superconductor resulting in an enhanced I_c of ZNWs. Indeed the resistance shows a drop from 1.0 to 0.35 Ω when the field is increased from below to above H^d.

In an In/ZNWs/In system with 2 μm long, 40 nm diameter ZNWs, complete suppression on superconductivity of ZNWs is found when the In electrodes are in the superconducting state.[9] *R*-*H* curves at 0.47 K show an abrupt switching of R from the superconducting to the normal value precisely, i.e., within 5.0 Oe, at the critical field of In electrodes without any evidence of a decoupling field H^d. Interestingly, the evidence of an H^d and a minimum in R between H^d and H_c of In is found in an In/ZNWs/In system with 6 μm long ZNWs that exhibits partial suppression of superconductivity. Figure 7(a) shows *R*-*H* scan at 10 nA well below the critical current of the ZNWs at different temperatures of this system. A locally enlarged part of this plot is shown in Fig. 7(b). This system is labeled as sample *Z*3 in Ref. 9 and the *R*-*T* and *V*-*I* curves of this system were presented in Fig. 3 of Ref. 9. Similar to the scans in Fig. 6, the *R*-*H* scans of Fig. 7 below 0.7 K also exhibit a minimum just below the critical field of In at 0.27 kOe. The field at which R begins to drop is 0.25 kOe. If we identify 0.25 kOe as H^d, then the magnetic field range of the minimum in R in the In/ZNWs/In system is many times narrower than that shown in Figs. 5 and 6 for the Pb/ZNWs/Pb system. It is not unreasonable to speculate that even for systems that exhibit complete suppression, there may also exist a very narrow region of magnetic field between H^d and H_c, where R will exhibit a minimum. This region may be so narrow that it has so far escaped detection because of limited resolution in H of our system (the smallest step we can change in magnetic field is 5 Oe).

IV. DISCUSSIONS

To date, the APE effect has been seen in 40 nm ZNWs with different bulk superconducting electrodes. This effect is unlikely to be an artifact due to electrical noise or other instrumental effects. In Ref. 9 we pointed out that we found identical suppression effects when the measurements were made with and without RF filters. It is also very difficult to explain the observation that the strength of the APE is material dependent based on the electrical noise mechanism.

Our data on the Pb/ZNWs/Pb system suggest that at zero or low magnetic fields the superconducting order parameter of the ZNWs is strongly coupled and affected by the superconducting order parameter of the Pb electrodes resulting in an anomalously low critical current. When the magnetic field is increased towards a value that is close to the critical field of Pb, the superconductivity of Pb electrodes is weakened and thus reduces the influences of the electrodes on the ZNWs leading to the striking recovery of the critical current shown in Fig. 4. What is missing in this qualitative explanation is the exact microscopic mechanism of APE between the electrodes and the ZNWs. We will consider below a number of theoretical models that seem relevant to our experiment.

Transport property of a model system consisting of a mesoscopic superconducting grain coupled by Josephson junctions to two macroscopic superconductors were considered theoretically by Refael and collaborators.[34] The system can go from a phase that is fully superconducting to one that is fully normal depending on the total shunting resistance of the two junctions. This model resembles, to some degree, the results presented above. However, in our case, the shunting or the interface resistances between the nanowires and bulk electrodes are much smaller than the "quantum" resistance $R_Q=h/4e^2=6.5$ $k\Omega$ considered in the model. The length of our Zn nanowires is more than 13 times longer than the superconducting phase coherence length of ZNWs, which is far from a grain being considered in the model.

Theoretical work by Buchler *et al.*[27] investigated the conductance and quantum fluctuations in a thin superconducting nanowire of finite length coupled to the environment through appropriate boundary conditions. They found that the environment plays a crucial role on the conductance of the wire and changes the phase diagram of the system at $T=0$ K. The disappearance of the superconductor to the insulator quantum phase transition and its resurrection due to the wire's

coupling to its environment is characterized through the dimensionless shunt's conductance $K=R_Q/R_p$, where $R_Q=6.5\ k\Omega$ is again the quantum resistance in 1D and R_p the shunt resistance of the environment acting on the device. When $K<1$ (i.e., $R_Q<R_p$), a nanowire of finite or infinite length both is in insulating and/or metal state. In the case of $K>1$ (i.e., $R_Q>R_p$), the nanowire is always in superconducting phase. Quasi-long-range order and stiffness of superconducting order parameter survives at $T=0$ K for an infinite or a finite wire when $K>1$. In our system, the shunting resistance is much smaller than the quantum resistance with $K\gg1$ because the resistances of an individual ZNW ($\sim250\ \Omega$), the electrodes and the interface resistance ($<20\ \Omega$), are also much smaller than the R_Q at 6.5 $k\Omega$. The observed APE cannot be explained by this model.

Martin-Rodero *et al.*[35,36] developed a self-consistent theory consisting of a narrow superconducting channel coupled to two wider superconducting electrodes. Wires of different lengths L are considered in this superconducting mesoscopic weak-link model. Our system resembles the theoretical case of $L\gg\xi_0$. In this limit the theory predicts the existence of a well-defined core region of length $\sim\xi_0$ at the center of the channel away from the electrodes. In the core region, the superconducting order parameter is nearly zero at $T=0$ K and the phase shows an abrupt change, in other words, a phase-slip center at zero bias voltage. This profile will lead to a very low value of the critical current and a finite resistance at the core region. This model seems to be relevant to our observation in Pb/ZNWs/Pb systems. However, there is no provision in this model for the complete destruction of superconductivity in the 1D channel as we have observed in the Sn/ZNWs/Sn and In/ZNWs/In systems. The channel material in the model is the same as the bulk electrodes and the amplitude of the order parameter on the constriction is the same as its bulk value of the electrodes. It would be interesting to extend this model to a system where the narrow channel is made of a different material from the electrodes.

Very recently, Fu *et al.*[28] developed a theory for a superconducting nanowire coupled to various environments. This theory considered the boundary effect and phase-slip interaction in the presence of dissipative environment and suggested that the APE is due to the dissipation at the boundary between the ZNWs and the electrodes. When the nanowire of finite length is placed into a dissipation free environment, the ends of the wire can be mapped onto two parallel boundary lines that can screen the vortex-antivortex interaction of the superconducting order parameter and destroys the superconducting phase even at $T=0$ K. When the ends of the wire are coupled to a dissipative environment (such as normal metal electrodes), the screening becomes incomplete. As a result, for sufficiently large dissipation the superconducting phase of the wire is stabilized. Because a quantum wire can undergo depairing when the phase fluctuation is severe, the model of Fu *et al.* did not require the normal state resistance of a quantum wire exceeding the quantum resistance. This theory is qualitatively consistent with a number of the experimental observations. However, this model does not address the observation that the "strength" of APE is dependent on the materials of the superconducting electrode materials.

The ratio of the superconducting gap (2Δ) to the transition temperature (T_c), $2\Delta/kT_c$, measures the strength of the electron-phonon interaction of a superconductor. The value of $2\Delta/kT_c$ is 3.5 for Sn, 3.6 for In, and 4.3 for Pb. Thus, the strength of the APE qualitatively varies "inversely" with the strength of the electron-phonon interaction.[37] We do not have an explanation for this correlation.

The APE has been observed only in zinc nanowires. In our extensive study on Sn wires, no evidence of APE was seen. We have made transport measurements on Sn nanowires with various lengths (6–35 μm) and diameters (20–100 nm) sandwiched between Sn electrodes.[19] This may be due to the fact that Sn nanowires have a short coherence length, $\sim$55 nm. Further work on shorter and thinner Sn nanowires may be interesting. Experiments on other wires with a long coherence length such as Al may also be revealing. These experiments are in progress.

V. CONCLUSION

Superconductivity of ZNWs of 40 nm in diameter and two micrometers in length $[L>\xi(0)]$ sandwiched between bulk superconductor Pb was investigated. Suppression of superconductivity of ZNWs by bulk Pb superconducting electrodes is found in the form of reducing the critical current of the Zn nanowires under low magnetic fields This critical current is found to begin to recover when the field is increased to a characteristic decoupling field H^d below the critical field of the Pb electrodes.

ACKNOWLEDGMENTS

We acknowledge helpful discussions with J. Clarke, A. M. Goldman, J. K. Jain, D. H. Lee, P. A. Lee, Y. Liu, T. E. Mallouk, and M. Tinkham. This work was supported by the Center for Nanoscale Science (Penn State MRSEC) funded by NSF under Grant No. DMR-0213623.

[1] G. E. Blonder, M. Tinkham, and T. M. Klapwijk, Phys. Rev. B **25**, 4515 (1982).
[2] H. Courtois, Ph. Gandit, and B. Pannetier, Phys. Rev. B **52**, 1162 (1995).
[3] P. Xiong, G. Xiao, and R. B. Laibowitz, Phys. Rev. Lett. **71**, 1907 (1993).
[4] A. F. Andreev, Zh. Eksp. Teor. Fiz. **46**, 1823 (1964) [Sov. Phys. JETP **19**, 1228 (1964)].
[5] D. Agassi and J. R. Cullen, Phys. Rev. B **54**, 10112 (1996).
[6] K. K. Likharev, Rev. Mod. Phys. **51**, 101 (1979).
[7] A. A. Golubov, M. Yu. Kupriyanov, and E. Il'ichev, Rev. Mod. Phys. **76**, 411 (2004).

[8] M. Tinkham, *Introduction of Superconductivity*, 2nd ed. (McGraw-Hill, International Edition, New York, 1996), p. 196.
[9] M. L. Tian, N. Kumar, S. Y. Xu, J. G. Wang, J. S. Kurtz, and M. H. W. Chan, Phys. Rev. Lett. **95**, 076802 (2005).
[10] H. Wang, M. M. Rosario, N. A. Kurz, B. Y. Rock, M. Tian, P. T. Carrigan, and Y. Liu, Phys. Rev. Lett. **95**, 197003 (2005).
[11] D. Y. Vodolazov, F. M. Peeters, L. Piraux, S. Matefi-Tempfli, and S. Michotte, Phys. Rev. Lett. **91**, 157001 (2003).
[12] S. Michotte, S. Matefi-Tempfli, L. Piraux, D. Y. Vodolazov, and F. M. Peeters, Phys. Rev. B **69**, 094512 (2004).
[13] F. Sharifi, A. V. Herzog, and R. C. Dynes, Phys. Rev. Lett. **71**, 428 (1993).
[14] P. Xiong, A. V. Herzog, and R. C. Dynes, Phys. Rev. Lett. **78**, 927 (1997).
[15] A. V. Herzog, P. Xiong, and R. C. Dynes, Phys. Rev. B **58**, 14199 (1998).
[16] A. Rogachev and A. Bezryadin, Appl. Phys. Lett. **83**, 512 (2003); A. Rogachev, A. T. Bollinger, and A. Bezryadin, Phys. Rev. Lett. **94**, 017004 (2005).
[17] A. T. Bollinger, A. Rogachev, M. Remeika, and A. Bezryadin, Phys. Rev. B **69**, 180503(R) (2004).
[18] A. Bezryadin, C. N. Lau, and M. Tinkham, Nature (London) **404**, 971 (2000).
[19] M. L. Tian, J. G. Wang, J. S. Kurtz, Y. Liu, and M. H. W. Chan, Phys. Rev. B **71**, 104521 (2005); M. L. Tian, J. G. Wang, J. Snyder, J. Kurtz, Y. Liu, P. Schiffer, T. E. Mallouk, and M. H. W. Chan, Appl. Phys. Lett. **83**, 1620 (2003).
[20] C. N. Lau, N. Markovic, M. Bockrath, A. Bezryadin, and M. Tinkham, Phys. Rev. Lett. **87**, 217003 (2001).
[21] M. Zgirski, K. P. Riikonen, V. Touboltsev, and K. Arutyunov, Nano Lett. **5**, 1029 (2005).
[22] F. Altomare, A. M. Chang, M. R. Melloch, Y. G. Hong, and C. W. Tu, Phys. Rev. Lett. **97**, 017001 (2006).
[23] N. Giordano, Phys. Rev. Lett. **61**, 2137 (1988); Phys. Rev. B **41**, 6350 (1990); **43**, 160 (1991).
[24] J. S. Langer and V. Ambegaokar, Phys. Rev. **164**, 498 (1967); D. E. McCumber and B. I. Halperin, Phys. Rev. B **1**, 1054 (1970).
[25] A. D. Zaikin, D. S. Golubev, A. van Otterlo, and G. T. Zimanyi, Phys. Rev. Lett. **78**, 1552 (1997).
[26] D. S. Golubev and A. D. Zaikin, Phys. Rev. B **64**, 014504 (2001).
[27] H. P. Buchler, V. B. Geshkenbein, and G. Blatter, Phys. Rev. Lett. **92**, 067007 (2004).
[28] H. C. Fu, A. Seidel, J. Clarke, and D. H. Lee, Phys. Rev. Lett. **96**, 157005 (2006).
[29] S. Sachdev, P. Werner, and M. Troyer, Phys. Rev. Lett. **92**, 237003 (2004).
[30] http://www.2spi.com/catalog/spec_prep/filter6.html
[31] M. L. Tian, J. G. Wang, J. Kurtz, T. E. Mallouk, and M. H. W. Chan, Nano Lett. **3**, 919 (2003).
[32] J. G. Wang, M. L. Tian, N. Kumar, and T. E. Mallouk, Nano Lett. **5**, 1247 (2005).
[33] C. Kittel, *Introduction to Solid State Physics*, 7th ed. (John Wiley & Sons, New York, 1996), p. 336.
[34] G. Refael, E. Demler, Y. Oreg, and D. S. Fisher, Phys. Rev. B **68**, 214515 (2003).
[35] A. Martin-Rodero, F. J. Garcia-Vidal, and A. Levy Yeyati, Phys. Rev. Lett. **72**, 554 (1994).
[36] A. Levy Yeyati, A. Martin-Rodero, and F. J. Garcia-Vidal, Phys. Rev. B **51**, 3743 (1995).
[37] This observation was made by M. Tinkham.